Dynamic Monte Carlo simulations of anisotropic colloids

Sara Jabbari-Farouji and Emmanuel Trizac

Citation: J. Chem. Phys. **137**, 054107 (2012); doi: 10.1063/1.4737928
View online: http://dx.doi.org/10.1063/1.4737928
View Table of Contents: http://jcp.aip.org/resource/1/JCPSA6/v137/i5
Published by the American Institute of Physics.

Dynamic Monte Carlo simulations of anisotropic colloids

Sara Jabbari-Farouji and Emmanuel Trizac
LPTMS, CNRS and Université Paris-Sud, UMR8626, Bat. 100, 91405 Orsay, France

(Received 20 April 2012; accepted 3 July 2012; published online 2 August 2012)

We put forward a simple procedure for extracting dynamical information from Monte Carlo simulations, by appropriate matching of the short-time diffusion tensor with its infinite-dilution limit counterpart, which is supposed to be known. This approach – discarding hydrodynamics interactions – first allows us to improve the efficiency of previous dynamic Monte Carlo algorithms for spherical Brownian particles. In the second step, we address the case of anisotropic colloids with orientational degrees of freedom. As an illustration, we present a detailed study of the dynamics of thin platelets, with emphasis on long-time diffusion and orientational correlations. © *2012 American Institute of Physics*. [http://dx.doi.org/10.1063/1.4737928]

I. INTRODUCTION

Monte Carlo (MC) simulations provide a powerful method for calculating the thermodynamical averages of physical quantities of many-body systems and have been employed to study the equilibrium properties and phases of a large variety of physical systems. Such approaches rely on the generation of a Markov chain – a stochastic set of configurations – with appropriate sampling of phase space. In the most common variants of MC, such as Metropolis algorithms, trial moves are accepted with a certain probability that satisfies detailed balance with respect to the desired Boltzmann distribution.[1,2] This method is frequently used to obtain average values of macroscopic quantities in equilibrium thermodynamic ensembles. Also, other variants of MC such as hybrid MC (Ref. 3) based on evolution of Hamiltonian have been devised that allow for global moves such as cluster moves to speed up the equilibration of the system. Thus, such schemes are more efficient for obtaining the ensemble averages of desirable quantities.

Although MC methods were initially devised to study static properties. In some cases though, where mesoscopic degrees of freedom interact with microscopic ones, the ensuing separation of time scales allows to replace the microscopic details by a noise, in the spirit of a Langevin equation. A suitably chosen MC scheme – stochastic in nature – then allows to study dynamical features of the mesoscopic degrees of freedom, meaning that correlations between successive configurations in the Markov chain of the MC simulation can be interpreted in terms of the dynamic correlation functions. The legitimacy of this approach stems from the coincidence of the Fokker-Planck equations of the original system governed by the aforementioned Langevin-type dynamics, and of the fictitious MC dynamics.[4–6]

Recently, there has been a rise of interest to employ MC simulations to study the dynamics of colloidal suspensions.[5,7,8] On the time scale that momenta correlations have decayed, colloids undergo diffusive motion as a result of collisions with solvent molecules. Therefore, at these time scales the stochastic dynamics generated by MC algorithm seems to be more appropriate compared to the deterministic Newtonian dynamics where solvent is omitted. Dynamic (sometimes known as Brownian) Monte Carlo (DMC) algorithms in which only single particle moves with sufficiently small displacements are allowed, excluding MC variants such as hybrid MC schemes, reproduce the real dynamics for times larger than the time scale of momenta relaxation. In such a case MC schemes *with physically meaningful moves* become equivalent to Brownian dynamics (BD) simulations:[4–13] a BD algorithm is also stochastic, with integrated out momenta and positions evolving with overdamped Langevin dynamics.[1] The advantage of DMC over BD is that it is easily adaptable to systems with non-differentiable (hard) potentials. Although an "event-driven" variant of BD technique has been developed[14] to deal with such types of interactions, the implementation of MC scheme is simpler. Furthermore, for the case of interacting particles, in BD simulations forces in each direction should be calculated while in MC simulation only energy needs to be computed. Hence, studying the dynamics of hard particles with the DMC scheme seems to be an efficient route, provided that an accurate mapping between the Monte Carlo time step and the physical time is worked out. Achieving this goal is the main motivation of the present work.

The significance of establishing the matching of time scales is justified by the recent increasing use of DMC for studying dynamics of various systems.[15–18] Recently, it has been proposed that equating the square of amplitude of MC displacement scaled with acceptance probability with infinite-dilution limit diffusion coefficient provides a good estimate of the physical time for spherical particles.[7] The applicability of this proposition is justified through agreement of BD simulations results with those of DMC.[7,8] Furthermore, these studies show that scaling the Monte Carlo time step with acceptance probability allows one to extend the limit of validity of DMC to relatively larger displacement amplitudes corresponding to acceptance probabilities – the fraction of accepted MC attempted moves – significantly smaller than 1. Here, we propose an alternative physically motivated approach for mapping the MC time to physical time. It allows us to push the limit of applicability of DMC to even larger displacement amplitudes (smaller acceptance probabilities). Our scheme is

based on equating the short-time self-diffusion extracted from simulations directly with the infinite-dilution diffusion coefficient. Particular attention is paid to anisotropic particles. At variance with previous approaches that did not consider the anisotropy of the short-time diffusion tensor,[8] we have taken into account the important coupling between orientational and translational degrees of freedom. In all what follows, the various short-time diffusion constants are supposed to be known, and implicitly account for the presence of an underlying solvent.

The rest of the paper is organized as follows. In Sec. II, the method is presented, for both spherical and anisotropic particles. In particular, we discuss the relation between the amplitudes of translational and rotational moves, essential to achieve a physically consistent diffusive process. In Sec. III, we study the convergence and self-consistency of DMC simulations as a function of displacement amplitude for both spherical and disk-shaped particles, and compare our approach with previous investigations. As an illustration, the method is employed in Sec. IV to explore the development of long-time translational diffusion of infinitely thin hard disks (platelets) as a function of density. We find that upon increasing the density deep in the nematic phase, the long-time diffusion becomes anisotropic, and that in contrast to an impeded diffusion in the nematic direction, the transverse diffusion of disks is enhanced. Concluding remarks close the paper with Sec. V.

II. METHODOLOGY

We start by describing the dynamic Monte Carlo algorithms used for both spherical and anisotropic particles. In each case, we discuss the procedure for matching of the time scales. We then introduce the model systems and provide the simulation details.

A. DMC algorithm for spherical particles

Colloids suspended in a solvent undergo overdamped Brownian motion with diffusive behavior, for large enough times compared to the momentum relaxation time τ_M^t. The latter quantity is set by the colloids mass M and the translational friction coefficient γ_t that depends on the particle size and shape, its value being $3\pi\eta\sigma$ for spherical objects of diameter σ with stick boundary conditions: $\tau_M^t \equiv M/\gamma_t$. The resulting mean-squared displacement (MSD) of non-interacting colloids varies linearly with time for $t \gg \tau_M^t$, with a slope given by the infinite-dilution diffusion coefficient $D_0^t = k_B T/\gamma_t$. However, for interacting colloids in non-dilute suspensions, different diffusion processes should be distinguished, namely, short-time D_S^t and long-time D_L^t diffusion. The distinction requires the introduction of the Brownian time scale τ_B defined as the time required for an isolated colloid to diffuse over its diameter σ, i.e., $\tau_B \equiv \sigma^2/(6D_0^t)$. For relatively short times, larger than τ_M^t but smaller than the Brownian time scale, the colloids influence each others motions indirectly through the solvent flow field in which they move. These solvent mediated hydrodynamic interactions may affect the short-time diffusion. If one ignores the hydrodynamic interactions, as in the subsequent analysis, the short-time diffusion is that of infinite-dilution diffusion coefficient $D_s^t = D_0^t$.[19,20] On the contrary, the long-time diffusion D_L^t that is defined for $t \gg \tau_B$ is mainly determined by the direct interactions between colloids.[19,21] For typical colloids with diameters in the range 10 nm–1 μm, we have $\tau_B/\tau_M^t \gg 1$ with well separated diffusive regimes.

Now, consider a MC procedure discarding hydrodynamic interactions, where each of N interacting spherical particles in the simulation box is shifted by a random displacement chosen in the interval $[-\delta l, \delta l]$ along each Cartesian coordinate. The moves are accepted according to the Metropolis algorithm.[2] Such a simulation mimics the Brownian motion of the colloids for time scales $t \gg \tau_M^t$. One expects that the MSD of a particle after n cycles $\langle \Delta r^2(n)\rangle = 1/N \sum_{i=1}^{N} \langle |\vec{r}_i(n) - \vec{r}_i(0)|^2\rangle$ varies linearly with the number n of MC cycles, for both small values of n corresponding to the short-time regime, and large n, albeit with a different slope. The MSD for sufficiently small n is governed by the infinite-dilution diffusion coefficient D_0^t, i.e., $\langle \Delta r^2(n)\rangle \approx 6D_0^t(n\delta t)$, provided that the amplitude of MC move δl is chosen sufficiently small, i.e., $\delta l \ll \sigma$ where δt is the physical time interval that each MC cycle corresponds to. As a result, we impose that the relation between the MC clock and the real time δt can be obtained from the slope of MSD in the small n limit, i.e., the short-time diffusion of MC simulation

$$\frac{\delta t}{\tau_B} = \lim_{n\to 0} \frac{\langle \Delta r^2(n)\rangle}{n\sigma^2}, \tag{1}$$

where $\lim_{n\to 0}$ with n an integer refers to the limiting behavior of the MSD slope at small n. It has been noted that for sufficiently small δl, $\langle \Delta r^2(1)\rangle = A\delta l^2$, where A is the acceptance probability of the MC scheme.[7] It was therefore suggested that the time scale corresponding to a MC cycle can be obtained as: $\delta t = A\delta l^2/6D_0^t$. Scaled in terms of Brownian time, this equation can be written as

$$\frac{\delta t}{\tau_B} = A\frac{\delta l^2}{\sigma^2}, \tag{2}$$

which provides an alternative route against which our approach will be tested in Sec. III. In the following, we will denote this A-rescaling procedure as the variant V_A, while the diffusion matching will be referred to as variant V_D. We will show that, quite expectedly, both methods become equivalent, for sufficiently small δl. However, enforcing (1) instead of (2) allows us to extend the limit of applicability of DMC towards larger values of δl.

B. DMC algorithm for anisotropic particles

For anisotropic particles with orientational degrees of freedom and depending on the shape, the diffusion in some directions is favored over some others, leading to the coupling of translational and rotational motions.[22] Henceforth, for a meaningful dynamics, due account should be taken of the anisotropy of diffusion in the body frame. Similar to the translation-only case, simulations based on DMC can produce the correct dynamics of the rotational degree of freedom for time scales larger than the damping time of angular velocity

$\tau_M^r = I_r/\gamma_r$, where I_r is the moment of inertia and γ_r is the rotational friction coefficient. The exact value of τ_M^r depends on the size, shape of the particle, and the axis of rotation under consideration, but its order of magnitude is the same as τ_M^t. On the other hand, the time scale for orientational relaxation τ_r is given by the inverse of the infinite-dilution rotational diffusion coefficient $D_0^r = k_B T/\gamma_r$ leading to $\tau_r/\tau_M^r = k_B T/I_r \gg 1$ for sufficiently large colloids.

To illustrate the DMC implementation for anisotropic colloids, we focus here on axially symmetric particles, although the generalization of our method to less symmetric objects is straightforward. We consider a system of N thin disks. Each of them can be identified by its center of mass position $\vec{r}_i$ and its orientation unit vector $\widehat{u}_i$ that is taken along the symmetry axis. The translational (resp. rotational) diffusion tensor in the body frame is diagonal and consists of one coefficient $D_{0||}^t$ (resp. $D_{0||}^r$) for the direction parallel to $\widehat{u}_i$ and two identical coefficients $D_{0\perp}^t$ (resp. $D_{0\perp}^r$) for perpendicular directions. In the following, we describe two variants of the same MC algorithm that consists of simultaneous translational and rotational displacements enforcing proper symmetry of the diffusion tensors. We ignore the rotations around the symmetry axis of the particle, as they cannot be detected in most of experiments; only rotations around axes perpendicular to symmetry axis are considered, i.e., rotations of the orientation vector, characterized by the same coefficient $D_{0\perp}^r$ which for simplicity we denote as D_0^r. The first variant, V_A, bears similarities with the approach presented in Ref. 8 but differs in two respects: first, no fine tuning of translational and orientational moves are required here; second, we fully resolve the anisotropic dynamics at short times, which is an essential prerequisite for the study of phases with orientational order, such as nematic phases. The second variant is reminiscent of the method put forward above for spherical particles.

We start by considering the limit of small MC increments, for which acceptance probability of the move is close to unity. A general attempted translational move can be described by $\delta\vec{r}_i = \delta x\,\widehat{n}_{x\,i} + \delta y\,\widehat{n}_{y\,i} + \delta z\,\widehat{u}_i$, where $\widehat{n}_{x\,i}$ and $\widehat{n}_{y\,i}$ are two mutually perpendicular arbitrary unit vectors that are normal to $\widehat{u}_i$ as well, δz is a random number in the interval $[-\delta l, \delta l]$, and δx, δy are random numbers in the interval $[-\delta l', \delta l']$. For sufficiently small δl and $\delta l'$, the average MSD in the direction parallel to $\widehat{u}_i$ is $\langle \delta z^2\rangle \simeq \delta l^2/3$ and along perpendicular directions is $\langle \delta x^2\rangle = \langle \delta y^2\rangle \simeq \delta l'^2/3$. Imposing the symmetry of the diffusion tensor provides us with a relation between $\delta l'$ and δl , i .e.,

$$\frac{\delta l'}{\delta l} \approx \sqrt{\frac{D_{0\perp}^t}{D_{0||}^t}}. \tag{3}$$

In addition, in the short-time diffusion regime, we should have $\langle \delta z^2\rangle = 2D_{0||}t$, so that the time increment corresponding to one single MC cycle reads

$$\delta t = \frac{\langle \delta z^2(1)\rangle}{2D_{0||}^t}. \tag{4}$$

If the orientation distribution for the ensemble of disks is isotropic, a restrictive assumption, we have $\langle \delta r^2\rangle = 2D_{0\perp}\delta l'^2 + D_{0||}\delta l^2$. Defining the average translational diffusion as $D_0^t = (2D_{0\perp}^t + D_{0||}^t)/3$, the MSD can then be simplified to $\langle \delta r^2\rangle \approx \frac{D_0^t}{D_{0||}^t}\delta l^2$.

The change of orientation can be seen as a random rotational displacement with an angle $\delta\theta$ in the interval $[0, \delta\alpha]$, such that $\widehat{u}_i^{new}.\widehat{u}_i = \cos\delta\theta$, see Fig. 1(b) for an illustration. Such a rotation can be achieved as follows:[2,23] we generate a unit vector $\widehat{u}_i'$ with an isotropic random orientation and obtain the new orientation vector as

$$\widehat{u}_i^{new} = \mathcal{N}[(1-\delta\alpha)\widehat{u}_i + \delta\alpha\widehat{u}_i'], \tag{5}$$

where $\mathcal{N}$ ensures proper normalization. From this, one can calculate the correlation between the new and initial orientation vector in terms of $\delta\alpha$,

$$\begin{aligned}\langle \widehat{u}_i^{new}.\widehat{u}_i\rangle = F(\delta\alpha) &\equiv \frac{6+4(-3+\delta\alpha)\delta\alpha}{6(-1+\delta\alpha)^2} \qquad \delta\alpha < 0.5\\ &\simeq 1-\delta\alpha^2/3+2/3\delta\alpha^3 \qquad \delta\alpha \ll 1,\end{aligned} \tag{6}$$

where the average is taken over all the possible orientations of the random vector $\widehat{u}_i'$. Then the function $F(\delta\alpha)$ is obtained as $1/2\int_0^\pi \mathcal{N}(\delta\alpha, \cos\theta)[(1-\delta\alpha)+\delta\alpha\cos\theta]\sin\theta d\theta$. In addition, for the physical Brownian system under study, we have $\langle \widehat{u}(t).\widehat{u}(0)\rangle = \exp(-2D_0^r t)$,[24] so that we get from Eq. (6)

$$\delta t = -\frac{\ln(F(\delta\alpha))}{2D_0^r}. \tag{7}$$

In the limit of small $\delta\alpha$, the mean-squared angular displacement for diffusion of orientational vector can be obtained from Eq. (6): $|\langle \widehat{u}(\delta\alpha) - \widehat{u}(0)\rangle|^2 \equiv \langle \delta\theta^2\rangle \simeq 2\delta\alpha^2/3$ (for $\delta\alpha \ll 1$) that should be equal to $4D_0^r A\delta t$. The last step is to enforce consistency of time scales, equating the two relations for δt, i.e., Eqs. (4) and (7). Doing so, we obtain

$$\delta t = \frac{\delta l^2}{6D_{0||}^t} \tag{8}$$

and the following constraint between the amplitudes of translational and rotational moves:

$$\delta l = \sqrt{-3\ln(F(\delta\alpha))}\sqrt{\frac{D_0^r}{D_{0||}^t}}. \tag{9}$$

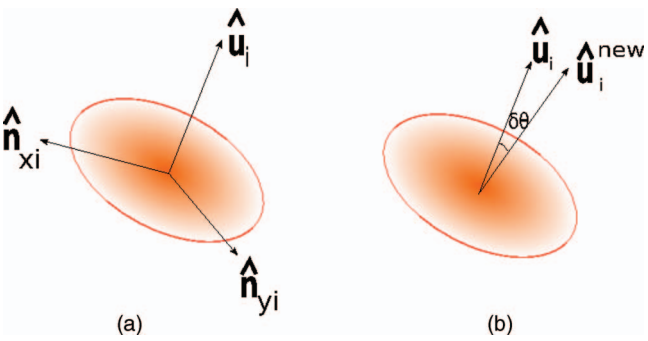

FIG. 1. A schematic drawing presenting (a) an example of an axially symmetric object with its orientation vector $\widehat{u}_i$ together with its body frame defined by $\widehat{u}_i$ and two mutually perpendicular vectors $\widehat{n}_{x\,i}$ and $\widehat{n}_{y\,i}$. (b) Rotation of orientation vector with an angle $\delta\theta$.

In the limit of smaller $\delta\alpha$, this simplifies into

$$\frac{\delta\alpha}{\delta l} \simeq \sqrt{\frac{D_0^r}{D_{0||}^t}}. \tag{10}$$

We should now take due account of the fact that $A \neq 1$. In the first variant of the approach, V_A, it is assumed that the physical time increment is slowed down by rejected moves, so that the generalized Eqs. (7) and (8) read

$$\delta t = A\frac{\delta l^2}{6D_{0||}^t} \tag{11}$$

$$\delta t = -A\frac{\ln(F(\delta\alpha))}{2D_0^r}. \tag{12}$$

Therefore, once the amplitude of orientational moves $\delta\alpha$ has been chosen, the amplitudes of translational moves δl and $\delta l'$ follow from Eqs. (3) and (9). Physical time is given by (11) or equivalently (12), where the acceptance probability A is computed on the fly in the simulation. Alternatively, for variant V_D, we again impose (3) and (9), but determine the physical time scale by imposing that $\langle \delta z^2(1)\rangle$ computed in the simulation coincides with $2D_{0||}^t t$.

Before illustrating the applicability of our DMC algorithm, we provide in the following section some details concerning the systems simulated.

C. Model systems and simulation details

In the remainder, we investigate the dynamics of two model systems by means of DMC simulations: hard sphere colloids (system A) and infinitely thin disks (system B) with diameters σ. We take into account the direct hard-core interactions by choosing at random a particle and generating a random trial MC move (including the rotational move for disks) and rejecting the displacements that lead to an overlap with neighbors.[23]

The first system consists of N spheres in a cubic box of length L, with periodic boundary conditions. We took $N = 1024$ and the simulations were performed for volume fractions $\Phi \equiv \pi\sigma^3/(6NL^3)$ in the range 0.05–0.5. The starting configuration was that of a Body-Centered Cubic (BCC) crystal melted by an equilibration run of 2×10^5 MC cycles (one trial move per particle). The production runs for calculating the mean-squared displacements consisted of $1 - 5 \times 10^6$ cycles, depending on the volume fraction and the amplitude of translational displacements $0.01 \leq \delta l/\sigma \leq 0.1$.

The second system consists of $N = 500$ disks again in a cubic simulation box with periodic boundary conditions. For each reduced density $\rho^* = N\sigma^3/L^3$, first an equilibration run of $5 - 10 \times 10^4$ MC cycles was performed starting with an initial configuration of disks on an FCC crystal with parallel orientations. The production runs for calculating the translational mean-squared displacements and orientational correlations were in the range of 10^6–10^7 cycles, depending on the density. The displacements amplitudes were in the range $2 \times 10^{-4} \leq \delta l/\sigma \leq 0.2$ and $0.005 \leq \delta\alpha \leq 0.324$. The infinite-dilution translational and rotational diffusion coefficients of disks used in the simulations are

$$D_{0||} = \frac{k_B T}{8\eta\sigma} \quad \text{and} \quad D_{0\perp} = \frac{3k_B T}{16\eta\sigma}, \tag{13}$$

giving an average diffusion coefficient of $D_0^t = \frac{k_B T}{6\eta\sigma}$. On the other hand, we have for the rotational diffusion

$$D_{0r} = \frac{3kT}{4\eta\sigma^3}. \tag{14}$$

These results are obtained from the general formula of diffusion coefficients of oblate spheroids[25,26] in the limit of vanishing length of semi-minor axis. Having described the methodology and simulation details, we present below the results of our DMC simulations.

III. ASSESSMENT OF THE DYNAMIC MONTE CARLO SCHEME

In this section, we present our DMC results for hard sphere self-diffusion, and then turn to thin disks. We compare and discuss the two different procedures for mapping MC time, i.e., rescaling with acceptance probability or directly matching short-time dynamics with infinite-dilution diffusion tensor.

A. Dynamics of spherical colloids

We start by discussing the time-scale matching in a colloidal suspension of hard spheres. Figure 2 shows the time dependence of the mean square displacement at a relatively high volume fraction $\Phi = 0.5$, for different values of MC displacement amplitude $\delta = \delta l/\sigma$. In Fig. 2(a), the physical time is obtained from δ^2 scaled with acceptance probability, i.e., $t/\tau_B = nA\delta^2$ as suggested in Ref. 7. As reported in Ref. 7 such a procedure leads to a decent data collapse, the goal being to obtain results that do not depend on δ. In this respect, the collapse is only partial, see, e.g., the $\delta = 0.1$ data that do not completely superimpose to those for $\delta = 0.01$.

In Fig. 2(b), we have obtained the physical time from the alternative method leading to Eq. (1). The graph shows that equating the short-time diffusion from MC with D_0^t directly, allows a better collapse of MSDs for larger values of δ (where acceptance probabilities are smaller). We emphasize that for the small $\delta = 0.01$, the two approaches yield the same results. However, with the present proposal, we can employ the DMC algorithm for relatively larger values of the increment δ. As discussed in Sec. II, the rationale behind our method is the fact that at short times ($t \ll \tau_B$), the particles diffuse freely with diffusion coefficient D_0^t, while for long enough times ($t \gg \tau_B$), the MSD crosses over from free diffusion to a slowed-down motion characterized by long-time diffusion D_L^t. This is illustrated in Fig. 3(a), for $\Phi = 0.5$, where the reduction of diffusion coefficients is ten-fold. These results provide us with a guideline for obtaining the optimal value of displacement for an efficient DMC scheme. It is the largest displacement δ for which we can still resolve the Brownian time scale, i.e., the short-time diffusion, where the corresponding mean-square displacement should correspond to that obtained for DMC of smaller amplitude (or BD if available).

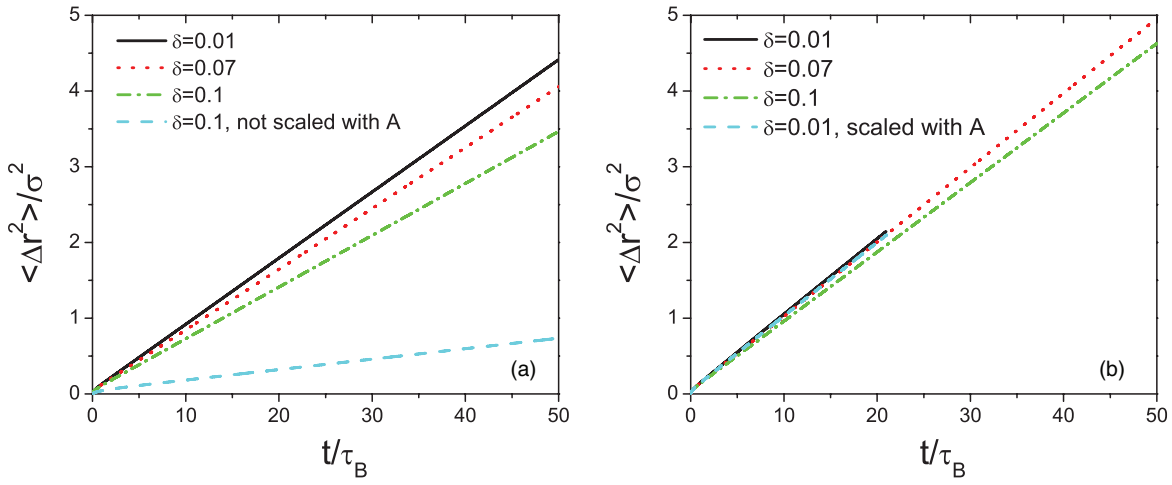

FIG. 2. Mean-squared displacement obtained from DMC simulations for a hard sphere system of volume fraction $\Phi = 0.5$, as a function of time. The curves correspond to three different values of displacement amplitude $\delta = \delta l/\sigma = 0.01$, 0.07, and 0.1. The corresponding acceptance probabilities A are: 0.84, 0.317, and 0.202, respectively. (a) t/τ_B is obtained by scaling with acceptance probability A using Eq. (2). The lower dashed curve shows the MSD data for $\delta = 0.1$ without A-rescaling. (b) t/τ_B is obtained from Eq. (1) by matching the MC short-time diffusion coefficient to D_0^t. For comparison, the curve with $\delta = 0.01$ and A-rescaling [i.e., the one shown in panel a)] is also plotted.

To further test the reliability of our method, we have plotted in Fig. 3(b) the long-time diffusion coefficient, extracted from the slope of the MSD curve at long times, as a function of volume fraction Φ for different sampling amplitudes. For comparison, we have also included the results obtained from scaling with A for $\delta = 0.1$ and Brownian dynamics results taken from Ref. 27. The simulation data from event-driven BD (Ref. 14) are fully consistent with our DMC results (not shown). While for $\delta = 0.01$ the two approaches are equivalent (as illustrated in Fig. 2(b)), some discrepancy is visible for $\delta = 0.1$ and $\Phi > 0.35$. We conclude here that the A-rescaling fares somewhat worse. For completeness, we also have displayed the theoretical results of Tokuyama and Oppenheim for the ratio of long-time to short-time diffusion D_L^t/D_S^t obtained for spherical particles when hydrodynamic interactions are accounted for. Good agreement is found with the present simulation data that discard such interactions, consistently with the findings of Ref. 21.

B. Dynamics of thin colloidal disks

We now turn to the DMC simulations of thin disks. First, we investigate the time behavior of MSD and orientational correlations for a low density system, and compare these results with the theoretical expectations for a freely diffusive particle. As can be seen in Fig. 4(a), the particles diffuse, as they should, with the same diffusion coefficient at short and long times. To quantify orientational dynamics, it is customary to define the correlation functions $\langle P_l(\widehat{u}_i(t) \cdot \widehat{u}_i(0))\rangle$,

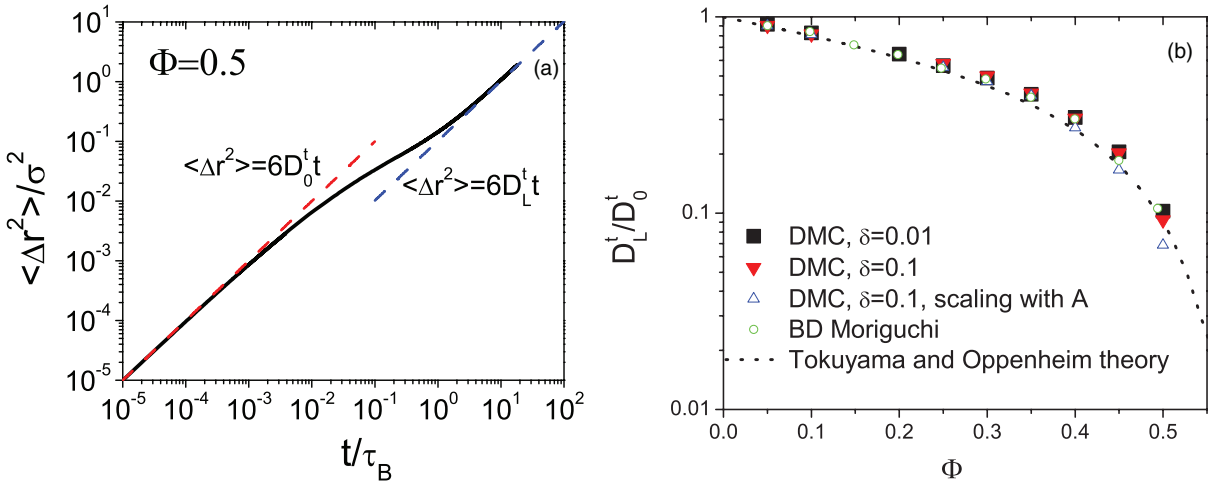

FIG. 3. (a) The mean square displacement obtained for $\Phi = 0.5$ and $\delta = 0.002$ clearly demonstrates a short-time slope of $6D_0^t$ (unity in scaled units) while at long time, the MSD grows with a reduced slope given by D_L^t. (b) Long-time diffusion coefficient of hard sphere colloids without hydrodynamic interactions, obtained from DMC simulations with two DMC variants: V_D (solid squares, $\delta = 0.01$, and triangle, $\delta = 0.1$) and V_A (open triangles, $\delta = 0.1$). Also shown are hard sphere BD results from Ref. 27 (open circles). The short-dashed curve is for the Tokuyama and Oppenheim formula,[28] that is used in Ref. 27 to obtain the ratio of long- to short-time diffusion.

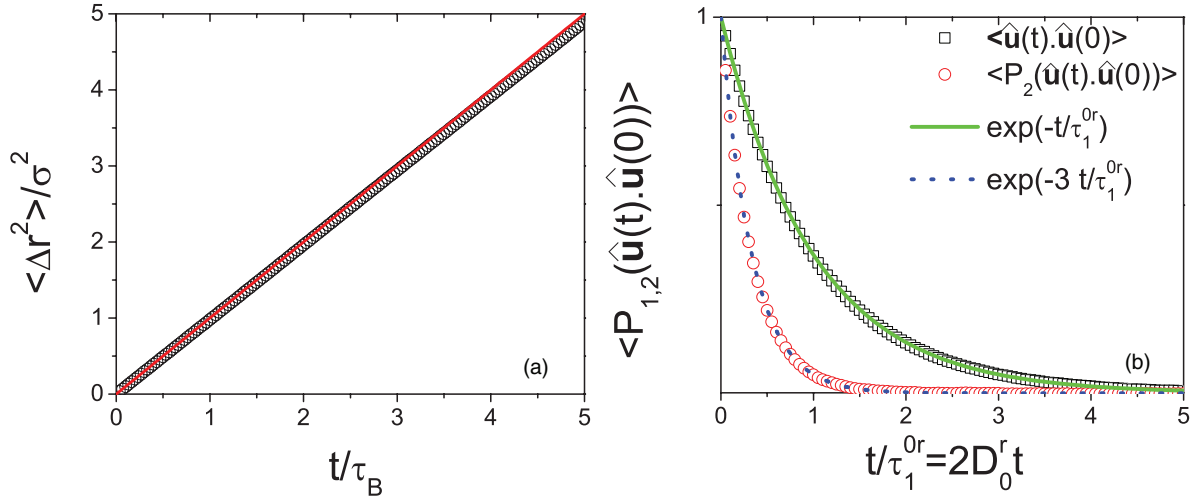

FIG. 4. DMC simulations results of thin platelets at a low density of $\rho^* = 0.1$, obtained for a displacement amplitude of $\delta = \delta l/\sigma = 0.005$, for which the acceptance probability is 0.9988. (a) The MSD as a function of $t/\tau_B = n\delta l^2$ agrees well with the line of slope unity. (b) The first- and second-order time orientational correlations versus $t/\tau_1^{0r} = 2nD_0^r\delta\alpha^2/3$ show a good agreement with $\exp(-t/\tau_l^{0r})$.

where P_l is the lth order Legendre polynomial. For a colloid in diluted conditions, these orientational time correlation functions decay exponentially with a relaxation time $\tau_l^{0r} = 1/(D_0^r l(l+1))$.[24,26] Of particular interest among the correlation functions are those associated with P_1 and P_2, that are related to the dielectric properties of polar liquids and to the scattering of depolarized light, respectively.[26] In panel (b) of Fig. 4, we have plotted both the first- and the second-order orientational correlation functions versus time. These functions show a very good agreement with their analytical infinite-dilution counterparts. It should be noted that with the parameters chosen in Fig. 4 where the acceptance ratio is close to unity, variants V_A and V_D coincide.

The next step is to explore the self-consistency of our two variants, where the time behavior generated should be independent of the auxiliary parameters chosen for MC sampling. We have one such parameter, say $\delta\alpha$, from which the other relevant increments δl and $\delta l'$ follow, see Eqs. (3) and (9). We first analyze the behavior of the translational self-diffusion. In Fig. 5, we have plotted the MSD of disks at a density $\rho^* = 2$, that is below the density of the isotropic-nematic transition $\rho^*_{IN} \simeq 4$,[23] as a function of physical time t/τ_B, for different MC sampling amplitudes. As discussed in Sec. II, we perform simultaneous translational and rotational moves. It appears that both variants V_A [with results shown in panel (a)] and V_D [results in panel (b)] are satisfactorily self-consistent, with a proper collapse of data. Nevertheless, it can be seen that variant V_A shows a somewhat smaller dispersion of results than that of V_D. Relatively large values of the sampling parameter are therefore acceptable, and provide results of a comparable accuracy as more demanding simulation with finer resolution. The analysis of orientational time correlations corroborates this conclusion, see Fig. 6. These conclusive tests allow us to study the density dependence of long-time diffusion in a

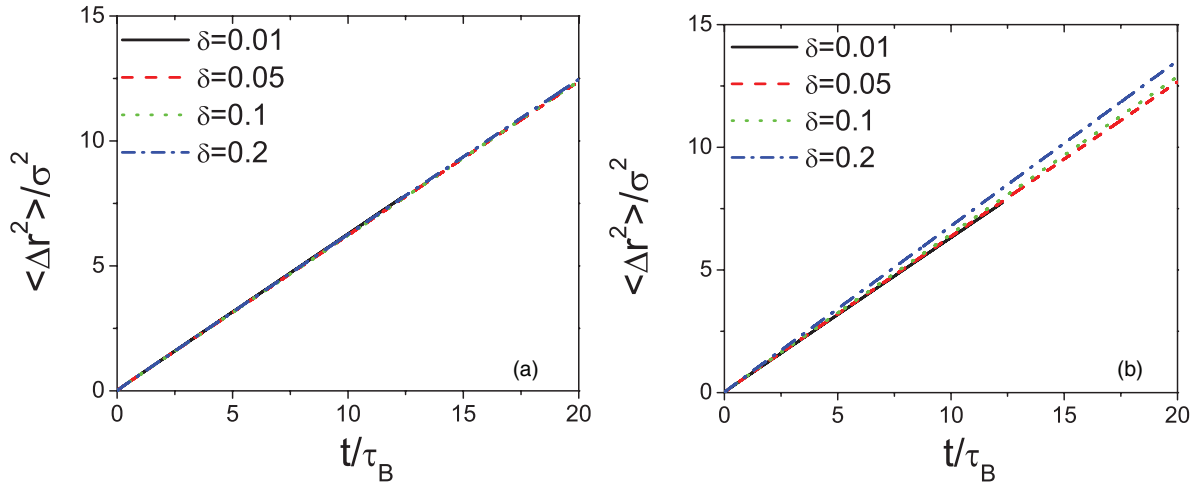

FIG. 5. Mean-squared displacement obtained from DMC simulations for infinitely thin platelets of reduced density $\rho^* = 2$, as a function of physical time. Different values of sampling amplitudes were used: $\delta = \delta l/\sigma = 0.01$, 0.05, 0.1, and 0.2 corresponding to $\delta\alpha = 0.0225$, 0.109, 0.196, and 0.324, respectively, and to the following acceptance probabilities: 0.93, 0.68, 0.48, and 0.25. (a) t/τ_B is given by variant V_A. (b) Results of variant V_D.

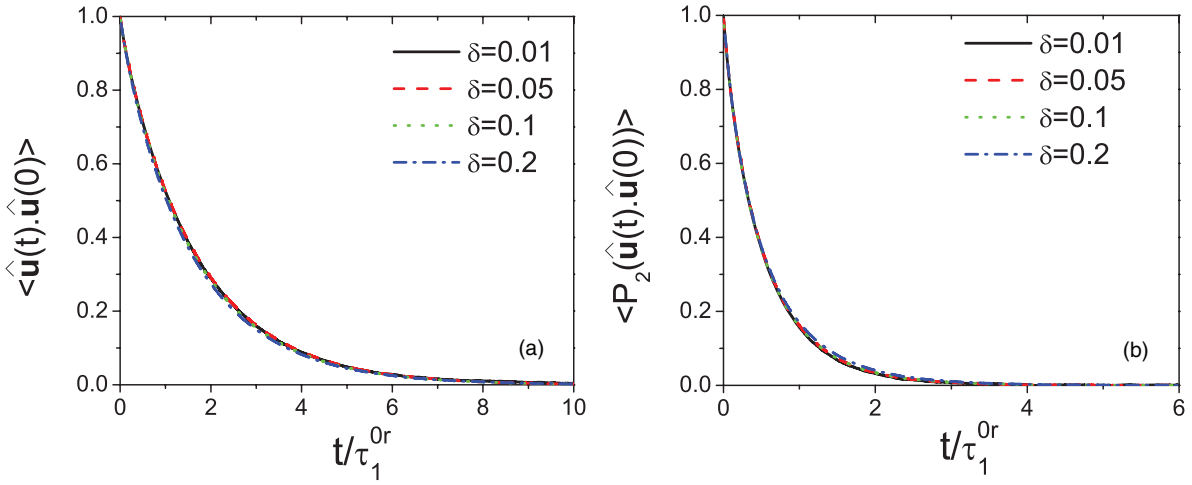

FIG. 6. Same as Fig. 5, for orientational correlations. In both cases, the results are reasonably independent of the sampling parameters.

system of disks, and in particular the effect of a phase transition crossing.

IV. ANOMALOUS DIFFUSION IN THE NEMATIC PHASE OF THIN DISKS

Thin platelets undergo an isotropic-nematic transition upon increasing the density,[23] and it is interesting to see how the long-time translational diffusion and orientational relaxation are affected. To this end, we have performed systematic DMC simulations with sufficiently small displacement amplitudes and have obtained both long-time translational self-diffusion coefficient and orientational relaxation time as a function of density. Figure 7(a) depicts the long-time translation self-diffusion coefficient D_L^t. We find that increasing the density, D_L^t decreases up to the transition point. However, in the nematic phase not only the short-time diffusion is anisotropic, but also the long-time diffusion becomes anisotropic with respect to the nematic director. Upon further increasing the density, we observe that the diffusion

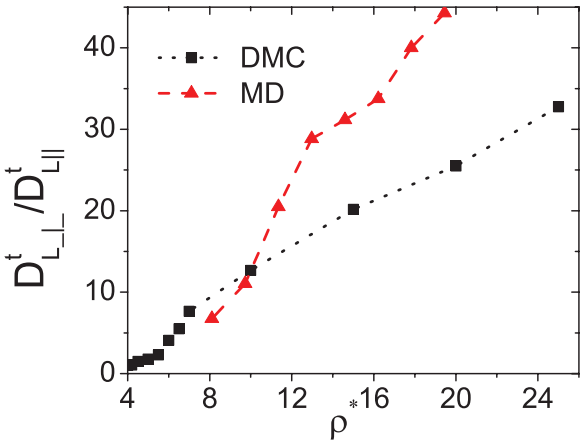

FIG. 8. Ratio $D_{L\perp}^t/D_{L\|}^t$ for hard disks as a function of density. DMC data are compared with their MD counterpart of Ref. 29.

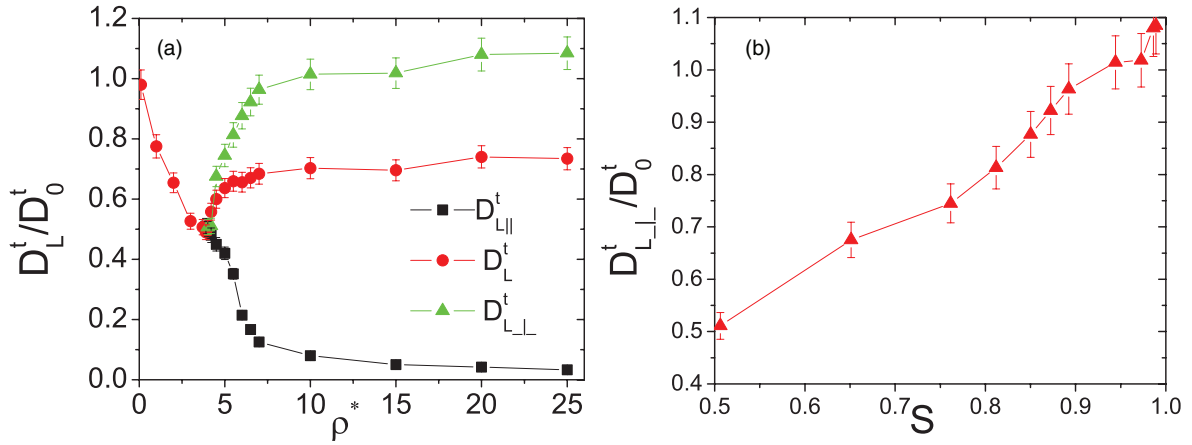

FIG. 7. (a) Long-time average diffusion coefficient D_L^t (in both isotropic and nematic phases) and long-time diffusion coefficients in directions parallel $D_{L\|}^t$ and perpendicular $D_{L\perp}^t$ to the nematic director for densities $\rho^* \geq 4$. (b) $D_{L\perp}^t$ as a function of nematic order parameter.

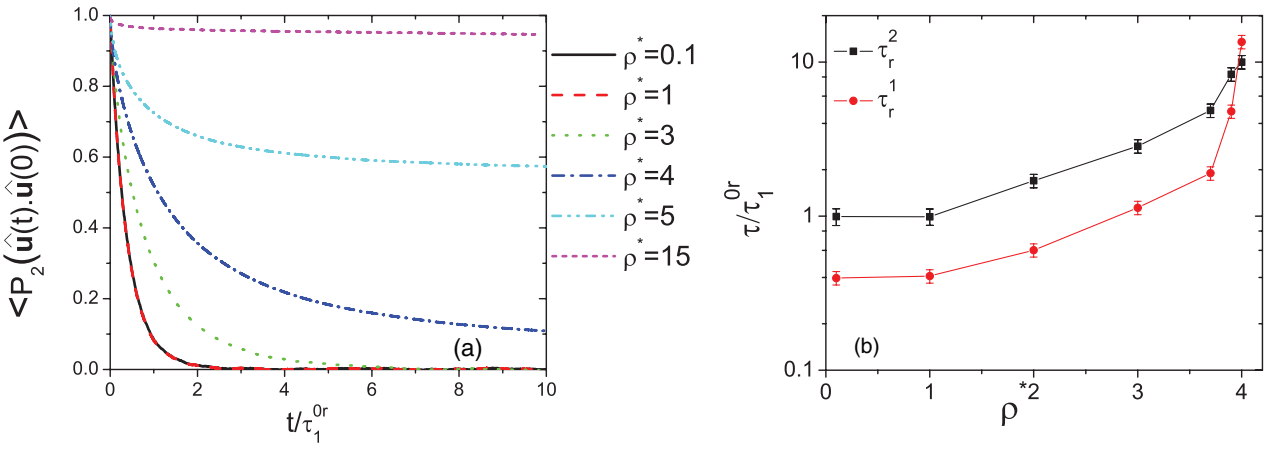

FIG. 9. (a) The second-order orientational correlation function for different densities of disks. (b) The first- and second-order rotational relaxation times in the isotropic phase, as a function of density.

coefficient in the direction perpendicular to nematic axis $D^t_{L\perp}$ grows while the parallel component $D^t_{L||}$ decreases significantly. As can be seen from Fig. 7(a), $D^t_{L\perp}$ approaches the free diffusion coefficient of disks $D^t_{0\perp}/D^t_0 = 9/8 = 1.125$ [see Eq. (13)] in the limit of very high densities. In Fig. 7(b), we have plotted $D^t_{L\perp}$ versus nematic order parameter S. As demonstrated by this figure the more the disks become aligned, the larger is the perpendicular component of the diffusion in contrast to $D^t_{L||}$ that becomes very small: topological constraints due to the excluded volume constrain the disks to move in a caging slab of parallel neighboring particles. We also emphasize that for all results presented in this section, variants V_A and V_D provide strictly identical results.

At this point it is interesting to compare our DMC results with molecular dynamics (MD) simulations of thin disks,[29] where an anisotropic diffusion in the nematic phase has also been observed.[29] However, one should keep in mind that the model in this work is not equivalent to ours. In our DMC simulations, we mimic the presence of an underlying solvent through the stochastic nature of MC moves. On the other hand, there is no solvent and hence the short-time diffusion is replaced by a ballistic regime in the MD approach of Ref. 29. For a quantitative comparison, Fig. 8 shows the ratio $D^t_{L\perp}/D^t_{L||}$ as a function of density. It seems that the two models have a different limiting behavior at high densities, where the MD data exhibit enhanced anisotropy.

We also have investigated the evolution of orientational time correlations with density, see Fig. 9(a). We observe that the orientational time correlations decay exponentially in the isotropic phase, while they become non-ergodic in the nematic phase and develop a plateau at long times whose value is equal to the square of nematic order parameter S. To quantify the development of relaxation time with density, we have fitted the orientational correlation functions in the isotropic phase with an exponential, and obtained the corresponding relaxation time for the first- and the second-order correlations as depicted in Fig. 8(b). As expected, relaxation times grow with density upon approaching the isotropic-nematic transition.

V. SUMMARY AND CONCLUSIONS

To summarize, we have presented a DMC algorithm for both spherical and anisotropic colloids. In each case, we have discussed the procedure for matching the Monte Carlo time scale with its physical counterpart. In the case of spherical particles, we found that matching the short-time diffusion from DMC to the infinite-dilution diffusion coefficient leads to a better convergence of results than acceptance rate based schemes, for relatively large values of displacement amplitude. A slightly better agreement of the long-time diffusion coefficient with Brownian dynamics data available in the literature was thereby achieved.

For anisotropic colloids, we presented two variants of the DMC algorithm that takes into account the anisotropy of short-time diffusion. As for spheres, one is acceptance-rate based (V_A), and one relies on short-time diffusion matching (V_D). Both routes are new in their present formulation, although variant V_A shares common features with the approach of Refs. 7 and 8. A key point is that the appropriate ratio of translational and rotational move amplitudes is enforced, which leads to the proper short-time diffusive behavior. We have tested the self-consistency of both variants that give similar results for a system of thin platelets in three dimensional space. The method was finally employed to investigate the evolution of the long-time diffusion coefficient and orientational correlation functions with density. The anisotropy of the long-time translational diffusion tensor was characterized in the nematic phase. While diffusion along the nematic axis becomes small when nematic ordering is more pronounced, it is enhanced in the perpendicular direction.

We also compared our results of anisotropic diffusion with previous MD simulations for platelets where an anisotropic long-time diffusion was observed as well.[29] Although the two sets of results agree qualitatively, a quantitative comparison is not possible as in this MD study the solvent-mediated Brownian effects were ignored. Therefore, it would be interesting to extend this study to systems such as soft disks where both BD and DMC simulations can be performed rather easily. Such a comparative study will provide an unambiguous validation of our proposed DMC method for

the anisotropic colloids. Another issue that deserves to be discussed at this point is the omission of hydrodynamic interactions in our DMC approach. In principle, our proposed DMC scheme can be modified to take into account hydrodynamic interactions as it is discussed for spherical particles by K. Kikuchi *et al*.[30]

ACKNOWLEDGMENTS

We wish to acknowledge the support of the Foundation Triangle de la Physiques and Intra-European Fellowship (IEF) Marie-Curie fellowship. We are also grateful to Patrick Davidson, Pierre Levitz, and Jean-Jacques Weis for fruitful discussions.

NOMENCLATURE

N	Number of particles in the simulation box of size L
M	Mass of particles
$\sigma = 2R$	Sphere or disk diameter
n	Number of Monte Carlo cycles, where a cycle is defined as one MC move per particle
$\Phi \equiv \pi\sigma^3/(6NL^3)$	Volume fraction of spheres
$\rho \equiv N/L^3$	Number density of thin disks
$\rho^* = \rho\sigma^3$	Dimensionless number density of thin disks
$\gamma_{t(r)}$	Translational (rotational) friction coefficient
$\tau_M^t = M/\gamma_t$	Time scale for which momenta of Brownian particles have relaxed
$\tau_M^r = I_r/\gamma_r$	Damping time of angular velocity for rotational Brownian particles
$D_0^t = k_BT/\gamma_t$	Infinite-dilution translational diffusion coefficient of spheres or average translational diffusion coefficient of anisotropic particles; for disks, we have $D_0^t = 2D_{0\perp}^t/3 + D_{0\|\|}^t/3$
D_S^t	Short-time translational diffusion coefficient
D_L^t	Long-time translational diffusion coefficient
$\tau_B \equiv \sigma^2/(6D_0^t)$	Brownian time scale, required for diffusing over a distance equal to the particle size
$D_{0\perp}^t = k_BT/\gamma_t^{\perp}$	Infinite-dilution translational diffusion of an axially symmetric particle in the direction perpendicular to the symmetry axis
$D_{0\|\|}^t = k_BT/\gamma_t^{\|\|}$	Infinite-dilution translational diffusion of an axially symmetric particle in the direction parallel to the symmetry axis
$D_{L\perp}^t$	Long-time translational self-diffusion of axially symmetric particles in the direction perpendicular to the nematic axis
$D_{\|\|}^t$	Long-time translational self-diffusion of axially symmetric particles in the direction parallel to the nematic axis
$D_{0\perp}^r \equiv D_0^r$	Infinite-dilution rotational diffusion of axially symmetric particle in the direction perpendicular to the symmetry axis; $\tau_r = 1/(2D_0^r)$ time scale for relaxation of orientation vector
$D_{0\|\|}^r = k_BT/\gamma_r^{\|\|} = k_BT/\gamma_r^{\perp}$	Infinite-dilution rotational diffusion of axially symmetric particle in the direction parallel to the symmetry axis.
$\langle \Delta r^2 \rangle$	Mean-square displacement (MSD)
$\langle \delta r^2 \rangle \equiv \langle \Delta r^2(1) \rangle$	Mean-square displacement after one MC step
$\langle \delta\theta^2 \rangle$	Angular mean-square displacement
A	Acceptance probability
δl	Amplitude of the translational displacement
$\delta = \delta l/\sigma$	
$\delta\alpha$	Maximal amplitude of the rotational displacement $\delta\theta$
δt	Physical time interval corresponding to one MC cycle
τ_l^r	The relaxation time of the orientational time correlation functions $\langle P_l(\widehat{u}(t) \cdot \widehat{u}(0)) \rangle$
$\tau_l^{0r} = 1/(l(l+1)D_0^r)$	The lth order orientational relaxation time of an isolated particle
S	Nematic order parameter

[1] M. P. Allen and D. J. Tildesley, *Computer Simulation of Liquids* (Oxford University Press, Oxford, 1987).
[2] D. Frenkel and B. Smit, *Understanding Molecular Simulation: From Algorithms to Applications*, 2nd ed. (Academic, 2001).
[3] S. Duane, A. D. Kennedy, B. J. Pendleton, and D. Roweth, Phys. Lett. B **195**, 216 (1987).
[4] K. A. Fichthorn and W. H. Weinberg, J. Chem. Phys. **95**, 1090 (1991).
[5] B. Cichocki and K. Hinsen, Physica A **166**, 473 (1990).
[6] K. Kikuchi, M. Yoshida, T. Maekawa, and H. Watanabe, Chem. Phys. Lett. **185**, 335 (1991).
[7] E. Sanz and D. Marenduzzo, J. Chem. Phys. **132**, 194102 (2010).
[8] F. Romano, C. De Michele, D. Marenduzzo, and E. Sanz, J. Chem. Phys. **135**, 124106 (2011).
[9] P. J. Rossky, J. D. Doll, and H. L. Friedman, J. Chem. Phys. **69**, 628 (1978).
[10] W. Schaertl and H. Sillescu, J. Stat. Phys. **74**, 687 (1994).
[11] D. M. Heyes and A. C. Branka, Mol. Phys. **94**, 447 (1998).
[12] S. Babu, J.-C. Gimel, T. Nicolai, and C. De Michele, J. Chem. Phys. **128**, 204504 (2008).
[13] H. F. Hernandez and K. Tauer, Comput.-Aided Chem. Eng. **25**, 769 (2008).
[14] A. Scala, T. Voigtmann, and C. De Michele, J. Chem. Phys. **126**, 134109 (2007).
[15] L. Berthier, Phys. Rev. E **76**, 011507 (2007).
[16] S. Belli, A. Patti, R. van Roij, and M. Dijkstra, J. Chem. Phys. **133**, 154514 (2010).
[17] A. Patti, S. Belli, R. van Roij, and M. Dijkstra, Soft Matter **7**, 3533 (2011).
[18] D. Coslovich, L. Strauss, and G. Kahl, Soft Matter **7**, 2127 (2011).
[19] G. Nagele, *The Physics of Colloidal Soft Matter*, Lecture Notes Vol. 14 (Institute of Fundamental Technological Research (AMAS), Warszawa, Poland, 2004), Chap. 9, p. 138.
[20] B. U. Felderhof and R. B. Jones, Phys. Rev. E **48**, 1084 (1993).
[21] M. Medina-Noyola, Phys. Rev. Lett. **60**, 2705 (1998).
[22] Y. Han, A. M. Alsayed, M. Nobili, J. Zhang, T. C. Lubensky, and A. G. Yodh, Science **314**, 626 (2006).
[23] R. Eppenga and D. Frenkel, Mol. Phys. **52**, 1303 (1984).
[24] J. Dhont, *An Introduction to Dynamics of Colloids* (Elsevier Science, 1996).
[25] F. Perrin, J. Phys. Radium **7**, 1 (1936).
[26] B. J. Berne and R. Pecora, *Dynamic Light Scattering*, 1st ed. (Dover, 2000).
[27] I. Moriguchi, J. Chem. Phys. **106**, 8624 (1997).
[28] M. Tokuyama and I. Oppenheim, Phys. Rev. E **50**, R16 (1994).
[29] A. Alavi and D. Frenkel, Phys. Rev. A. **45**, R5355 (1992).
[30] K. Kikuchi, M. Yoshida, T. Maekawa, and H. Watanabe, Chem. Phys. Lett. **196**, 57 (1992).